



## ORIGINAL ARTICLE

# Fluorescent pH probes for alkaline pH range based on perylene tetra-(alkoxycarbonyl) derivatives

Fengxia Zhang<sup>a</sup>, Wenyao Dong<sup>c</sup>, Yongshan Ma<sup>a,\*</sup>, Tianyi Jiang<sup>a</sup>, Bing Liu<sup>a,b</sup>, Xuemei Li<sup>a</sup>, Yuanyuan Shao<sup>a</sup>, Junsen Wu<sup>a</sup>

<sup>a</sup> School of Municipal and Environmental Engineering, Shandong Jianzhu University, Jinan 250101, Shandong, China

<sup>b</sup> Resources and Environment Innovation Research Institute, Jinan 250101, Shandong, China

<sup>c</sup> The First Clinical Medical College of Shandong University of Chinese Medicine, Jinan 250014, Shandong, China

Received 27 March 2020; accepted 30 April 2020

Available online 11 May 2020

## KEYWORDS

Perylene tetra-(alkoxycarbonyl) derivatives;  
Alkaline pH probe;  
Absorption spectrum;  
Fluorescence spectrum

**Abstract** The pH detection in the alkaline range is particularly important in many fields such as leather processing, waste water treatment, paper industry, and metal mining and finishing. Compared with traditional analysis methods such as colorimetric sensors and electrochemical sensors, the fluorescence and colorimetric probes for pH measurements have attracted much more attention due to their advantages of high sensitivity, excellent selectivity, noninvasiveness, low cost, fast response time, the possibility of continuously measurement, etc. However, there are few fluorescent probes fitting for alkaline pH monitoring. Actually, the design and synthesis of them were more significant for new probes producing. In this study, the design, synthesis, and practical application of two novel fluorescent pH probes for alkaline pH assay were discussed. Both of the two probes were derived from perylene tetra-(alkoxycarbonyl). The red or blue shift of the absorption/fluorescence spectrum was caused by the introduction of electron donor amino or oxygen ring in the bay region. Due to electronic separation of the OH group from the electron-withdrawing core, the probes have high pKa values and cover the pH range from 8 to 12. They exist in either fluorescent acid form or non-fluorescent basic form. It was investigated that the amino substituent at bay region had a higher pKa value than O-heterocyclic annulated perylene, which showed that the adjustable pKa value could be achieved by the modification of electron withdrawing groups. The probes would have a wide use for testing strips measurements and monitoring pH changes in concrete.

© 2020 The Author(s). Published by Elsevier B.V. on behalf of King Saud University. This is an open access article under the CC BY license (<http://creativecommons.org/licenses/by/4.0/>).

\* Corresponding author.

E-mail address: [mlosh@sdjzu.edu.cn](mailto:mlosh@sdjzu.edu.cn) (Y. Ma).

Peer review under responsibility of King Saud University.



Production and hosting by Elsevier

## 1. Introduction

As an important index of acidity, pH value is one of the most important parameters in chemical industry, biotechnology and environmental science (Gotor et al., 2017; Han and Burgess, 2010). Compared with normal pH probes, fluorescent pH sensor materials have attracted increasing attention due to their

high accuracies (Li et al., 2018; Lukinavicius et al., 2016). Fluorophores such as fluoresceins, perylenes, coumarins, cyanines, rhodamines, naphthalimides, and nile blue/red have been widely applied in the design of pH probes (Georgiev et al., 2019; Myochin et al., 2011; Sondergaard et al., 2015; Yuan et al., 2019). Most of these dyes were responded to pH changes in near neutral and acidic range, which facilitate their applications in biology, biotechnology, medicine, and environmental monitoring (Vanacek et al., 2018; Yin et al., 2015). However, fluorescent probes in response to alkaline pH range were relatively rare (Yang et al., 2019; Chai et al., 2015). Notably, the ability to sensing pH in alkaline range was particularly important in some fields such as leather processing, waste water treatment, paper industry, and metal mining and finishing (Horváth et al., 2019; Hecht et al., 2013). It was also critical for detection of corrosion of steel-reinforced concrete structures since the lifetime of these materials strongly depended on the internal pH value. Whereas, the pH value of concrete was generally ranged from 12.5 to 13.5 at the initial stage, while the alkalinity of the medium was gradually decreased and remained above pH 10 to maintain the steel components passive (Nguyen et al., 2014). So the durable and low-cost alkaline pH sensing materials were more valuable for the actual application (Staudinger et al., 2019).

In the past decades, perylene diimides (PDIs) showed a significant use due to their excellent chemical, photo, thermal, and weather stability (Rao et al., 2012; Li and Wonneberger, 2012; Sukul et al., 2014). However, many PDIs displayed the poor solubility and weak fluorescence, which limited their application (Wang et al., 2015; Wenger, 2011). Perylene tetra-(alkoxy carbonyl) derivatives (PTACs), similar in structure to PDIs and four electron deficient carboxylic ester groups attached, showed better solubility and excellent fluorescence in organic solvents (Marciniak et al., 2011; Ma et al., 2017). In order to further improve the performance of PTACs, substituted PTACs should be energetically developed.

Moreover, the electronic properties of PTACs could be fine-tuned by the substitution of the conjugated aromatic core (Chao et al., 2005). Many perylene bisimides with either electron-donating or electron-withdrawing groups have been reported (Aulin et al., 2018; Weitz et al., 2008). Perylene bisimides modified with electron-donating substituent have been characterized as near-infrared fluorescent dyes (Inan et al., 2017). This change may be caused by the electronic coupling between the electron-deficient perylene core and electron rich substituent, or substituent induced distortion of perylene core (Aigner et al., 2013; Zhang et al., 2018). In addition, the properties of perylene bisimides could also be adjusted by incorporating heteroatom to the perylene skeleton (Zhao and Han, 2009; Shoer et al., 2015; Ma et al., 2016). The introduction of four alkoxy carbonyl substituents at the imide-region of the perylene core broken down the original planar conformation of perylene and the photophysical properties of perylene was affected (Ma et al., 2017). Developing core-extended PTACs is a good approach to improve the optical and electronic properties of the PTACs. It was suggested that PDIs modified with oxygen cycle in the bay region could induce the perylene skeleton to remain planar form and cause hypsochromic shift of absorption spectrum (Ma et al., 2017).

In this study, two novel PTAC pH indicator dyes was presented: 1-amino-12-hydroxyl-tetra-(n-butoxyloxycarbonyl) perylene (probe **1a**) and 1-hydroxyl-mono-five-membered O-heterocyclic annulated tetra (n-butoxyloxycarbonyl) perylene (probe **1b**) (Scheme 1). The introduction of electron donor amino and electron accept oxygen ring in the bay region caused red and blue shift of the absorption/fluorescence spectrum for **1a** and **1b**, respectively. The probes show reversible “on”–“off” fluorescence response upon deprotonation of the receptor. The probes exist in either fluorescent acid forms or non-fluorescent basic forms. The optical properties of probes can be modulated by changing the balance between the two forms. We can imagine that the phenolic group will become phenol under acidic conditions. Due to the decreased internal charge transfer efficiency, the visible spectra will be blue shifted and the fluorescence enhancement can be observed. Due to electronic separation of the OH group from the electron-withdrawing core, the probes have significantly high pKa value and cover the pH range from 8 to 12. We can use this change in color and fluorescence emission to determine the pH value. In addition, the probes can be used for test strips measurement and monitoring pH in concrete.

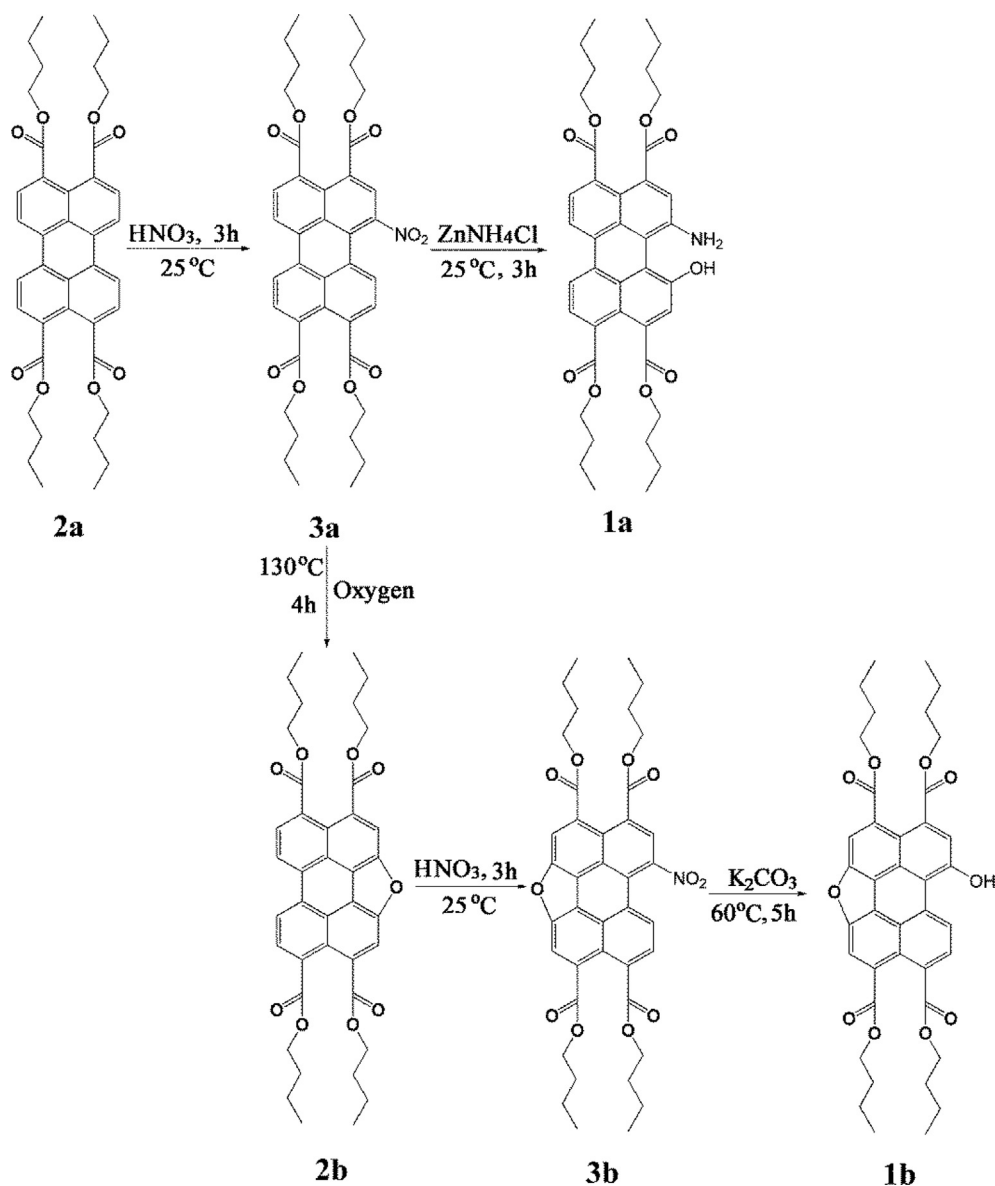
## 2. Experimental section

### 2.1. Materials

3,4,9,10-Perylenetetracarboxylic dianhydride was purchased from TCI (Shanghai, China). Sodium bicarbonate, nitric acid, dichloromethane, magnesium sulfate, ammonium chloride, zinc powder, tetrahydrofuran, methyl acetate, N-methylpyrrolidone and hydrochloric acid were of reagent grade and purchased from Aladdin (Shanghai, China), directly used without further purification. Detailed synthesis of probes **1a-b**, their spectral ( $^1\text{H}$  NMR,  $^{13}\text{C}$  NMR, and HRMS) and analytical characterization data were provided in the [Supplementary Information](#). Spectroscopic grade acetonitrile (purchased from Aladdin, Shanghai, China) were used throughout the detection experiments. Column chromatography was performed with silica gel (300–400 mesh).

### 2.2. Synthesis and structural characterization of probes **1a-b**

The synthetic routes of probes **1a-b** were presented in [Scheme 1](#). Compounds **2a-b** were facilely mononitrated with fuming nitric acid to give nitro compounds **3a-b**. Probe **1a** was obtained through a reduction reaction by reacting compound **2a** with ammonium chloride and zinc powder (Dubey et al., 2016; Gupta et al., 2015). Probe **1b** was prepared by using O-heterocyclic annulated tetra (n-butoxyloxycarbonyl) perylene (**2b**) as the starting reagent. **2b** was facilely mononitrated with fuming nitric acid to yield **3b**, which was then hydrolyzed to obtain probe **1b** with a high yield. Structural identity of all of the compounds was established by  $^1\text{H}$  NMR,  $^{13}\text{C}$  NMR, IR spectroscopy, and mass spectrometry (see [Supporting Information](#)). It could be seen that compounds **1a-b** consisted of a perylene dye fluorophore moiety and a hydroxy moiety.



**Scheme 1** Synthesis of probes **1a-b**.

### 2.3. Measurements and characterization

Absorption spectra were recorded on a Varian CARY-50 (America) spectrophotometer. Emission spectra and fluorescence quantum efficiency ( $\Phi_f$ ) were performed using Hitachi FL-4500 (Japan) spectrofluorometer.  $^1\text{H}$  NMR and  $^{13}\text{C}$  NMR spectra measurements were performed on a Bruker Advance 300 (Germany) spectrometer using TMS as internal reference. FT-IR spectra were measured on a Bruker Tensor-27 (Germany) spectrophotometer. Mass spectra were carried on a Bruker Maxis UHR-TOF (Germany) MS spectrometer. All the pH measurements were carried out with a Model PHS-3C (China) meter. Cyclic voltammetry (CV) were recorded on a CH 1604C (China) electrochemical analyzer at a potential rate of 200 mV/s in a solution of tetrabutylammonium hexafluorophosphate (TBAPF6) (0.1 M) in dichloro-

methane. Platinum, glassy carbon (diameter: 1.6 mm; area 0.02 cm<sup>2</sup>) and Ag/AgNO<sub>3</sub> electrodes were used as counter, working, and reference electrodes, respectively. The photos were taken on a Samsung GT-I8268 (korea) camera (f-number 2.7, exposure time 1/11 S, ISO-400, focal length 3 mm, maximum aperture 2).

## 3. Results and discussion

### 3.1. Photophysical properties

The optical properties of compounds **1a-b** and **2a-b** (Scheme 1) in acetonitrile were investigated by UV-vis absorption and fluorescence spectroscopy. As shown in Fig. 1(a), probe **1a** exhibited a maximum absorption at 503 nm, which was red shifted about 33 nm compared with compound **2a** (centered at

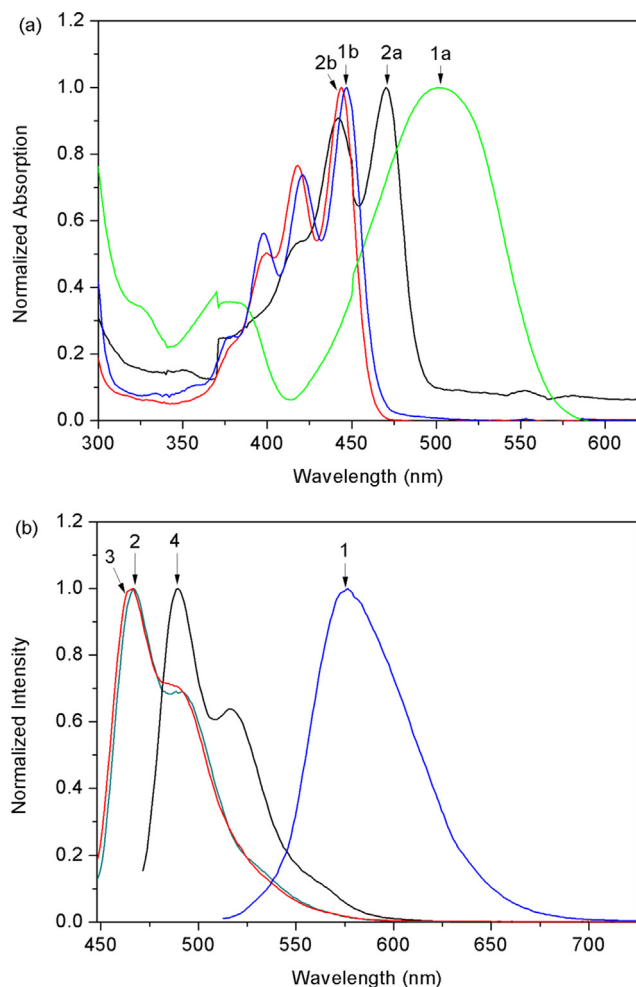


**Fig. 1** Normalized (a) absorption and (b) fluorescence spectra of compounds **1a-b** and **2a-b** in 10  $\mu$ M acetonitrile solutions.

470 nm). The two substituents (hydroxyl and amino) of **1a** comparatively increased the conjugation extent owing to the p-orbitals were more perpendicular to the naphthalene unit than that in **2a**. This conformation provided effective  $\pi$ -conjugation in the fused systems, and it resulted in a substantial red shift in the absorption spectrum of compound **2a** (Dubey et al., 2016). The spectrum of compound **2b** was blue-shifted about 22 nm relative to that of compound **2a** since the aromatic core was extended along the short molecular axis (Shoer et al., 2015). The longest maximum of compound **1b** (450 nm) was red-shifted relative to compound **2b**. This change may be caused by the electronic coupling between the electron-deficient perylene core and electron rich substituent, or substituent induced distortion of perylene core (Aigner et al., 2013).

The fluorescence spectra of compounds **1a-b** and **2a-b** in dichloromethane depict the same structure with approximate mirror images of the absorption spectrum, and the emission peaks appeared at 576 nm, 469 nm, 489 nm, and 467 nm for **1a**, **1b**, **2a** and **2b**, with corresponding Stokes shifts of 73 nm, 21 nm, 19 nm and 12 nm, respectively. This indicated that increase of Stokes shift owing to the introduction of hydroxyl or amino groups into the perylene core resulted in planar

distortions. The fluorescence quantum yield ( $\Phi_f$  **1a** = 0.49,  $\Phi_f$  **1b** = 0.69,  $\Phi_f$  **2a** = 0.72,  $\Phi_f$  **2b** = 0.78) in chloroform solution was measured using fluorescein as standard ( $\Phi_f$  = 0.85, 0.1 M NaOH) (Zhang et al., 2018). Clearly, the photophysical properties were affected strongly by modifying the hydroxyl, amino, and O-heterocyclic annulated substituent linking to the perylene core.

### 3.2. Electrochemical properties

The electrochemical property of compounds **1a-b** and **2a-b** have been investigated by cyclic voltammetry (Fig. 2). The compounds exhibited two irreversible oxidation and two quasi-reversible reductions waves. Compounds **1a-b** and **2a-b** showed two reduction peaks, implying their ability to accept at least two electrons. Table 1 summarized the redox potential, the lowest unoccupied molecular orbital (LUMO) and the highest occupied molecular orbital (HOMO) energy levels estimated from cyclic voltammetry. The HOMO/LUMO energy levels of compounds **1a-b** and **2a-b** were estimated to be  $-5.78/-3.65$ ,  $-6.12/-3.39$ ,  $-6.03/-3.86$ ,  $-6.17/-3.42$ , respectively.

### 3.3. Optical properties of the probes **1a-b** toward pH

Perylene bisimides modified with electron-donating substituent have been characterized as near-infrared fluorescent dyes (Inan et al., 2017). To meet the requirement for responding to pH in the long wavelength region, probe **1a** was synthesized with electron-rich amino and hydroxy in the perylene core. Thus, it exhibits red shifts in both absorption and emission spectra relative to those of probe **1b**. The pH-dependent spectral characteristics of probe **1a** (10 mM) were evaluated in acetonitrile (Fig. 3). There was a well-defined isobestic point at 533 nm in the absorption spectra, which indicated the presence of acid-base equilibrium between the two forms of probe **1a** (Scheme 1). In the acid form, probe **1a** had an absorption maximum at 503 nm (Fig. 3a) and an emission maximum at 582 nm (Fig. 3b). Meanwhile, pH titrations indicated that

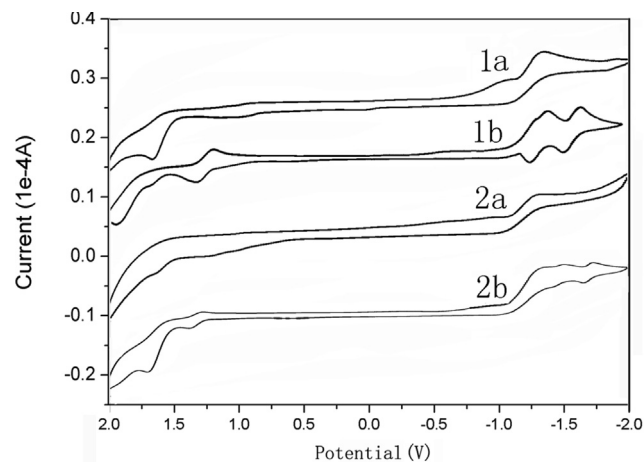


**Fig. 2** The cyclic voltammogram of compounds **1a-b** and **2a-b** (under  $N_2$  atmosphere, scanning rate 20 mV/s) using  $Bu_4NPF_6$  as electrolyte, glassy carbon electrode as work electrode, platinum as the counter electrode, and  $Ag/AgNO_3$  as reference electrode.

**Table 1** Cyclic voltammetry data and molecular orbital energies of compounds **1a-b** and **2a-b** with respect to the vacuum level.

Compound	$E_{\text{red1}}^0$ <sup>a</sup> (V)	$E_{\text{red2}}^0$ <sup>a</sup> (V)	$E_{\text{ox1}}^0$ <sup>a</sup> (V)	$E_{\text{ox2}}^0$ <sup>a</sup> (V)	HOMO/LUMO <sup>b</sup> (eV)	$E_{\text{gap}}^b$ (eV)
1a	$-1.15 \pm 0.02$	$-1.34 \pm 0.02$	$0.98 \pm 0.02$	$1.70 \pm 0.03$	$-5.78/-3.65$	2.13
1b	$-1.39 \pm 0.03$	$-1.65 \pm 0.02$	$1.30 \pm 0.03$	$1.64 \pm 0.05$	$-6.10/-3.41$	2.69
2a	$-0.94 \pm 0.02$	$-1.41 \pm 0.03$	$1.23 \pm 0.03$	$1.61 \pm 0.01$	$-6.03/-3.86$	2.17
2b	$-1.38 \pm 0.04$	$-1.51 \pm 0.02$	$1.37 \pm 0.01$	$1.69 \pm 0.02$	$-6.17/-3.42$	2.75

<sup>a</sup> Measured in a solution of 0.1 M tetrabutylammonium hexafluorophosphate (TBAPF<sub>6</sub>) versus Ag/AgNO<sub>3</sub> (in V),  $k = 2$ .

<sup>b</sup> Calculated from  $E_{\text{HOMO}} = -4.88 - (E_{\text{oxd}} - E_{\text{Fc/Fc}^+})$ ,  $E_{\text{LUMO}} = E_{\text{HOMO}} + E_{\text{gap}}$ .

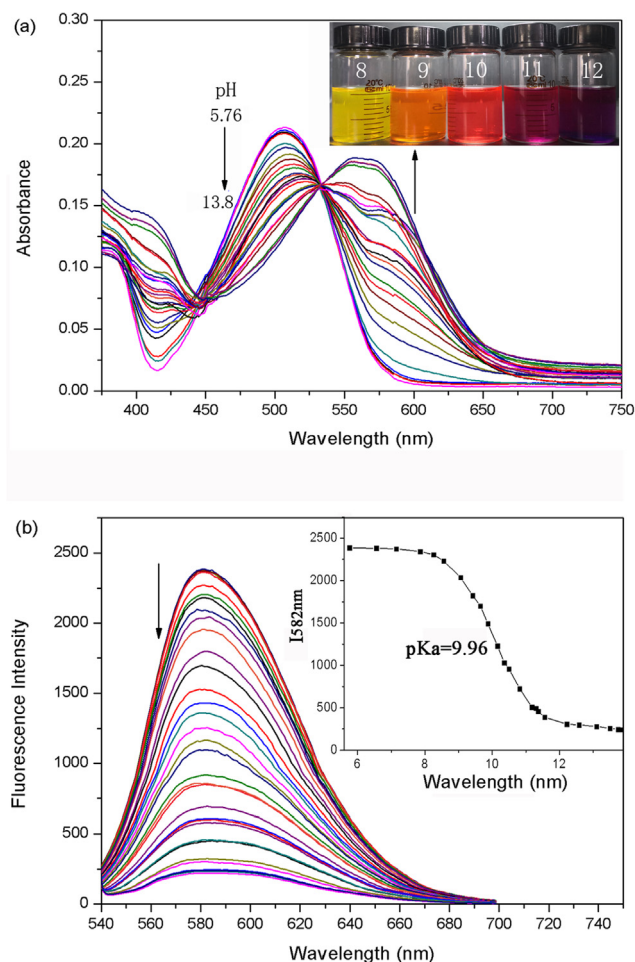


**Fig. 3** Absorption and fluorescence spectra of **1a** (10  $\mu\text{M}$ ) in acetonitrile at varied pH. (a) Absorption spectra. The inset shows pH-dependent photograph of the sample. (b) Emission spectra ( $\lambda_{\text{exc}} = 533 \text{ nm}$ ). The inset shows sigmoidal fitting of pH-dependent fluorescence intensity at 582 nm and pH-dependent photograph under UV light ( $\lambda_{\text{exc}} = 365 \text{ nm}$ ).

the base form of probe **1a** displayed red-shifted peak (563 nm) in the absorption spectrum and a significant fluorescence quenching response in the emission spectra, which can be explained by ICT (Intramolecular Charge Transfer) change in the basic and acidic conditions. The most likely explanation was that the O<sup>-</sup> atom on the bay-core was protonated in the acidic condition, so that charge transfer was no longer

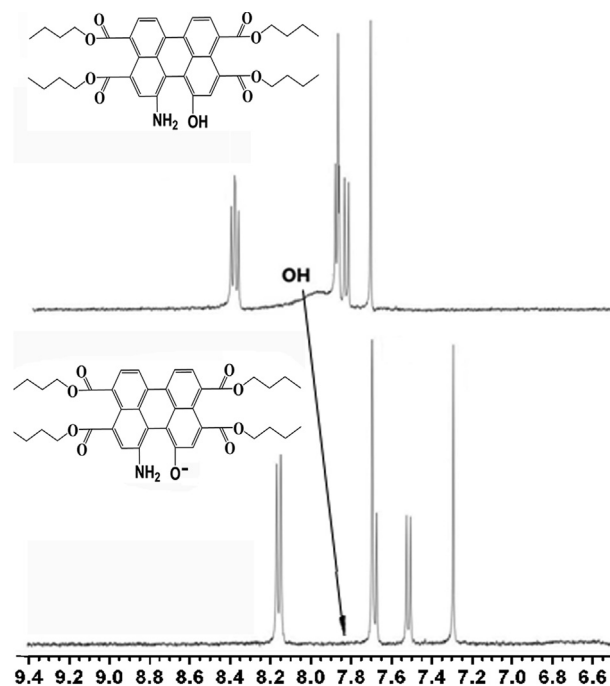


**Fig. 4** <sup>1</sup>H NMR spectral deprotonated and protonated changes of probe **1a** in CD<sub>3</sub>Cl<sub>3</sub>.

possible. Furthermore, a reversible protonation/deprotonation cycle has also been demonstrated. To verify the detection mechanism, the protonating and deprotonating processes were characterized by <sup>1</sup>H NMR spectra (Fig. 4). The low fields of <sup>1</sup>H NMR was totally changed from protonated structure to the deprotonated structure. A pKa value of 9.96 was obtained using the plot of the fluorescence intensity of I<sub>582 nm</sub> (Fig. 3b). Further proof regarding the equilibrium was obtained by observing obvious color change from yellow to magenta in visible light (Fig. 3a inset), and from brilliant yellow to dark red in ultraviolet light (Fig. 3b inset), when the pH increased. Notably, probe **1a** had large Stokes shifts (75 nm). Therefore, the detection sensitivity can be improved by a large Stokes shifts because of the reduced self-quenching and minimized measurement errors.

The optical properties of probe **1b** were similar to those of probe **1a**. Under neutral conditions, the blue-shifted absorption and emission maxima of compound **1b** (compared with **2a**) can be explained by the extended aromatic core along the short molecular axis (Shoer et al., 2015). As shown in Fig. 5a and b, the absorption wavelength was red-shifted from

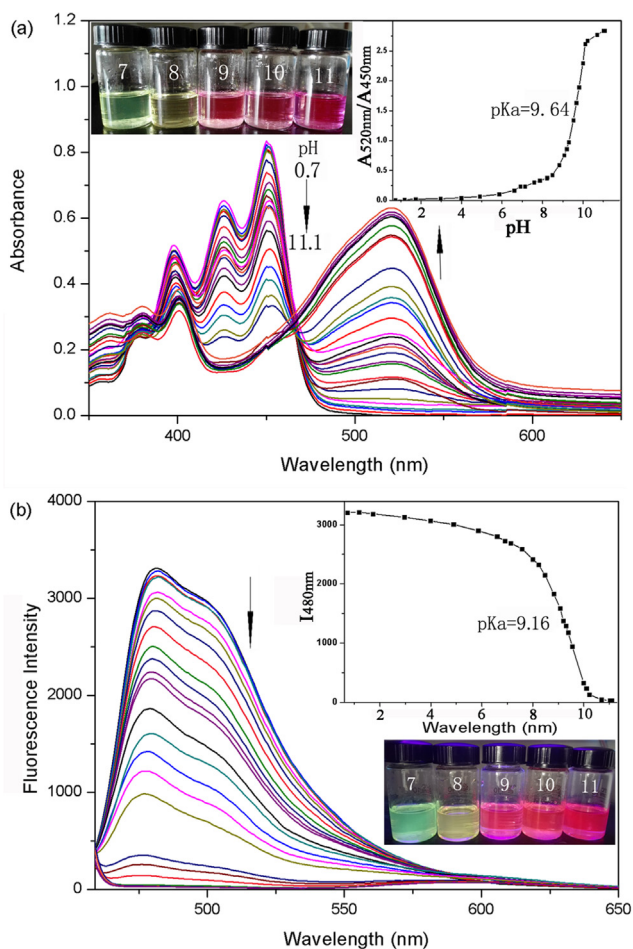


**Fig. 5** Absorption and fluorescence spectra of **1b** (30  $\mu\text{M}$ ) in acetonitrile with varied pH. (a) Absorption spectra. The inset shows a pH dependent plot of the absorbance ratios  $A_{520\text{nm}}/A_{450\text{nm}}$  and photograph of the sample. (b) Emission spectra ( $\lambda_{\text{exc}} = 466 \text{ nm}$ ). The inset shows sigmoidal fitting of pH-dependent fluorescence intensity at 480 nm and pH-dependent photograph under UV light ( $\lambda_{\text{exc}} = 365 \text{ nm}$ ).

450 nm (pH = 5) to 520 nm (pH = 11). A  $\text{pK}_a$  value of 9.64 was obtained by plotting the absorbance ratios  $A_{520 \text{ nm}}/A_{450 \text{ nm}}$ , and an isosbestic point at 466 nm was observed. The observed bathochromic shifts of the bands were due to the electron donor for  $\text{O}^-$  moiety was better than that for free  $\text{O-H}$  moiety. As a result, the solution color changed from blue-green to purple (Fig. 5a inset). Meanwhile, with the increase of pH value, the emission band centered at 481 nm decreased significantly and the fluorescence emission spectra showed a pronounced blue shift from 481 nm to 474 nm (pH > 10) (Fig. 5b). The blue shift of the signals could be assigned to the fluorescence of the deprotonated species. Sigmoidal fitting yields a  $\text{pK}_a$  value of 9.16, which is very close to that obtained from absorption measurements. It was obvious that the  $\text{pK}_a$  of **1b** decreased when the amino of **1a** was replaced by  $\text{O-}$  ring in the perylene core position. It was suggested that the adjustable  $\text{pK}_a$  could be achieved by the modification of ring groups. Further observation showed that the fluorescent blue-green of the solution faded away at pH 7 and 11. Probe **1b** showed

strong fluorescence in acidic and neutral solutions, but hardly in basic solutions (Fig. 5b inset).

### 3.4. Reversibility, selectivity, and aggregation assays of probes **1a-b**

It is well-known that reversibility of pH probe is highly required. When solutions containing probes **1a-b** were changed to low or high pH values by using concentrated hydrochloric acid and aqueous sodium hydroxide, no significant changes in emissivity were observed after 4 cycles (Fig. 6). The response and recovery time of different pH solutions were rapid. Meanwhile, the visual fluorescence color of solution changed between brilliant yellow (pH 6.0) and dark red (pH 12.0) for **1a**, and between blue-green (pH 7.0) and purple (pH 11) for **1b**. Both probe **1a** and **1b** obviously exhibited highly reversible responses to pH.

The selectivities of probes **1a-b** for preferential binding to  $\text{H}^+$  over other ions and biologically relevant analytes were also determined via absorption and fluorescence spectroscopy in acetonitrile. As shown in Fig. 7, probes **1a-b** was not

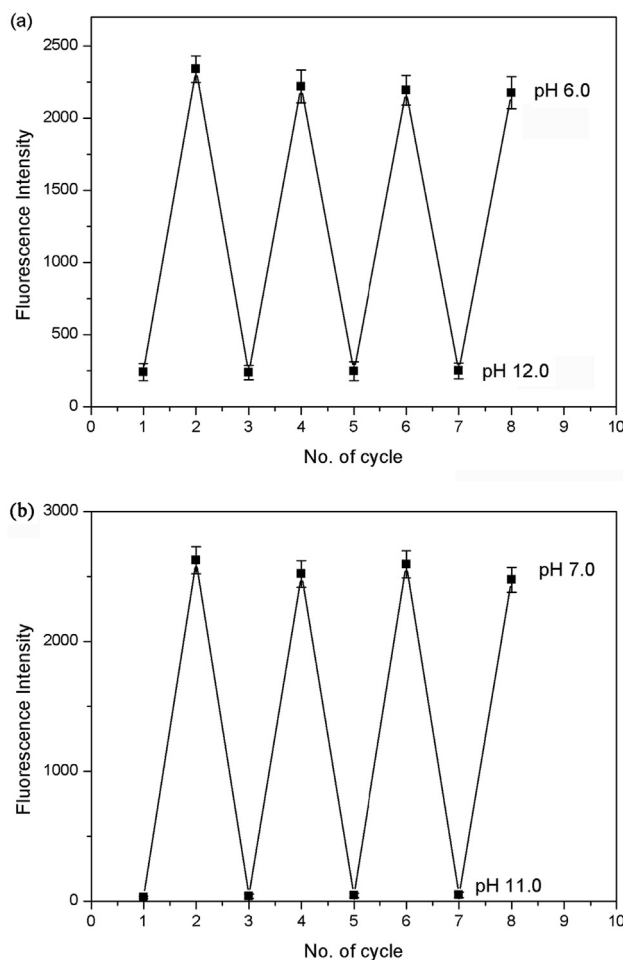


**Fig. 6** Reversible optical response of probes **1a-b** under alkaline and acidic conditions. (a) The emission ratios ( $I_{582 \text{ nm}}$ ) of probe **1a** at pH 6.0 and 12.0. (b) The emission ratios ( $I_{481 \text{ nm}}$ ) of probe **1b** at pH 7 and 11.

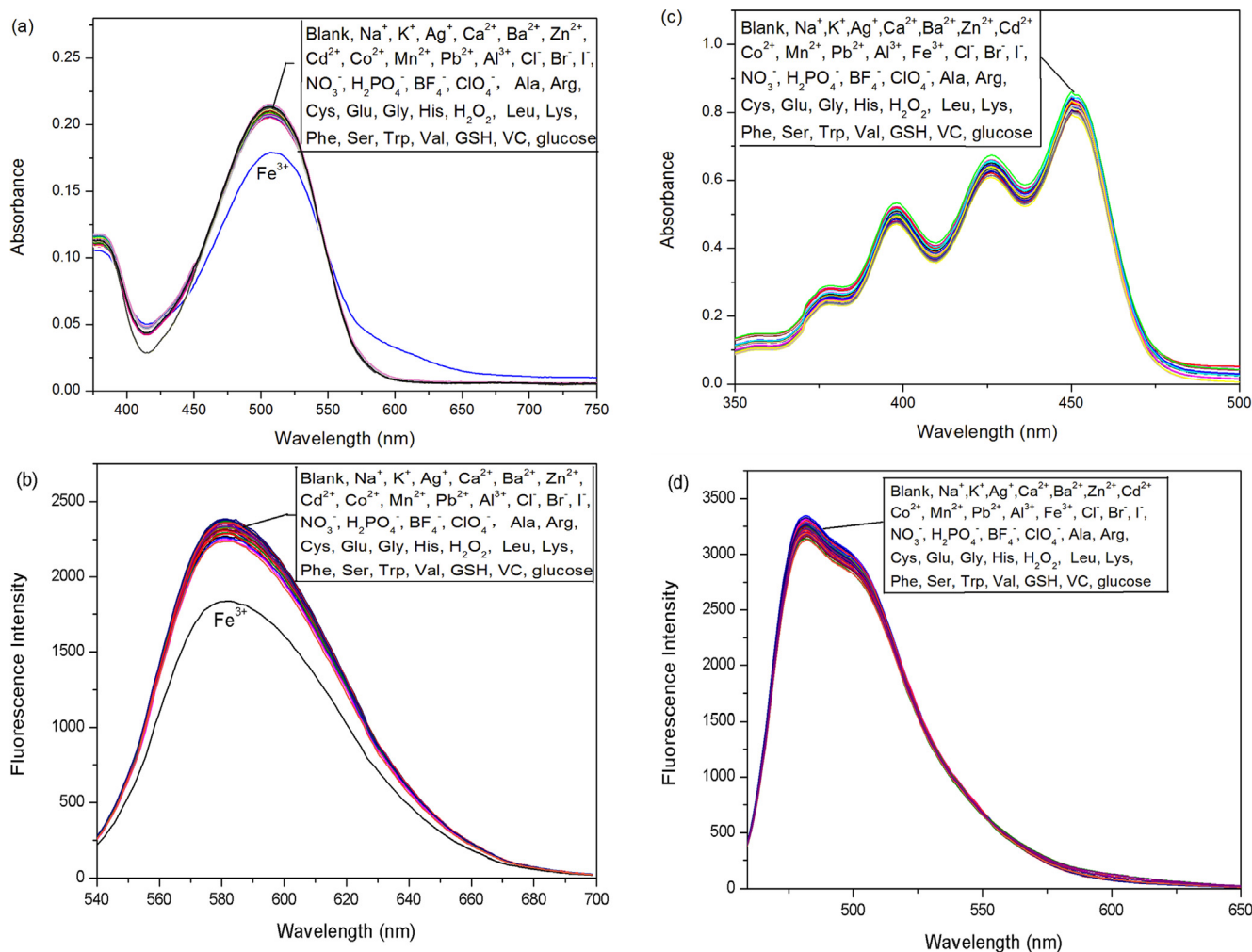


**Fig. 7** Absorption (a and c) and fluorescence (b and d) ( $\lambda_{\text{exc}} = 533$  nm for **1a**,  $\lambda_{\text{exc}} = 466$  nm for **1b**) response of probes **1a** (a and b) and **1b** (c and d) at pH 7 to 100 equiv of different ions and biologically relevant analytes.

sensitive to ions such as  $\text{Na}^+$ ,  $\text{K}^+$ ,  $\text{Mg}^{2+}$ ,  $\text{Ca}^{2+}$ ,  $\text{Ag}^+$ ,  $\text{Al}^{3+}$ ,  $\text{Ba}^{2+}$ ,  $\text{Cd}^{2+}$ ,  $\text{Co}^{2+}$ ,  $\text{Fe}^{2+}$ ,  $\text{Hg}^{2+}$ ,  $\text{Mn}^{2+}$ ,  $\text{Ni}^{2+}$ ,  $\text{Pb}^{2+}$ ,  $\text{Zn}^{2+}$ ,  $\text{Cl}^-$ ,  $\text{Br}^-$ ,  $\text{I}^-$ ,  $\text{NO}_3^-$ ,  $\text{H}_2\text{PO}_4^-$ ,  $\text{BF}_4^-$ ,  $\text{ClO}_4^-$ . In addition, various amino acids and biological reagents (Ala, Arg, Cys, Glu, Gly, His, Leu, Lys, Phe, Ser, Trp, Val, GSH, VC and Glu) also had little effects on the activity of probes **1a-b**.  $\text{Fe}^{3+}$  caused some variations in the absorbance and fluorescence since it can be complexed by probe **1a**. However, the low sensitivity limits its capability as a  $\text{Fe}^{3+}$  probe. The high selectivity and high reversible response to pH of probes **1a-b** made them promising candidates for developing practical pH sensors.

It is known that PDIs tend to aggregate in solution. Probes **1a-b** were structurally related to PDIs but have four alkoxy-carbonyl substituents at the imide-region of the perylene core. The concentration-dependent optical properties of probes **1a-b** were studied. As shown in Fig. 8, the absorption maxima of probes **1a-b** were linearly related to the concentration (5–40  $\mu\text{M}$ ). No obvious new peaks was found in the normalized absorption concentration curves. They showed excellent solubility in organic solvents because the four alkoxy-carbonyl substituents destroy the original planar conformation of perylene.

### 3.5. Quantum chemistry computation

To gain more insight into the mechanism of the coordination of probes **1a-b** with different pH value, quantum mechanical calculations were obtained on density functional theory (DFT) at the B3LYP/6-31G\* level. The molecular geometries in the ground state and the frontier molecular orbital of compounds **1a-b**, **1a<sup>-</sup>-b<sup>-</sup>** were shown in Fig. 9. According to the calculations, the optimized geometries of probes **1a-b**, **1a<sup>-</sup>-b<sup>-</sup>** had different core twist angles. Approximate dihedral angles between the two naphthalene subunits attached to the central benzene ring were calculated ( $15.69^\circ$  for **1a**,  $0.61^\circ$  for **1b**,  $15.61^\circ$  for **1a<sup>-</sup>**, and  $0.45^\circ$  for **1b<sup>-</sup>**). Four *n*-butoxyloxycarbonyl groups were attached to act as electron-accepting groups to induce ICT transition in **1a<sup>-</sup>-b<sup>-</sup>** that consisted of electron-donating ( $-\text{O}^-$ ) moieties and perylene moieties. The HOMO and LUMO orbital delocalized over whole perylene core evidently including the substituent of **1a<sup>-</sup>-b<sup>-</sup>**. The calculated HOMO-LUMO gaps (Table 2) of **1a**, **1a<sup>-</sup>**, **1b** and **1b<sup>-</sup>** were 2.47 eV, 2.20 eV, 2.78 eV and 2.38 eV, respectively.

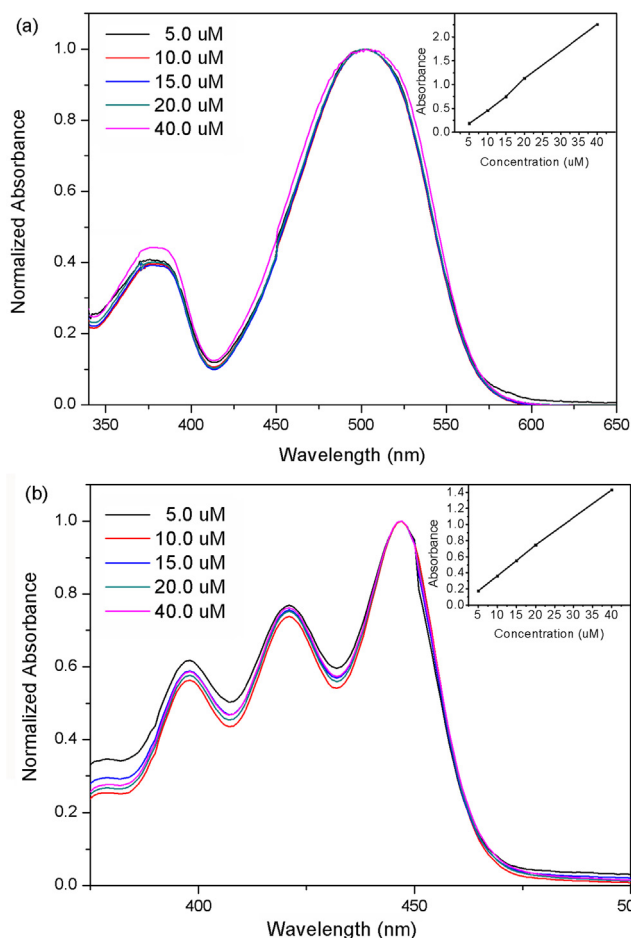


**Fig. 8** Normalized absorption spectra of probes **1a** (a) and **1b** (b) in acetonitrile. The insert show the linear relationship of absorption intensity and concentration.

### 3.6. Test strips measurement

In order to study the properties of the probes in practical applications, real-time measuring tapes for alkaline pH value was developed. A paste of probes **1a-b** in acetonitrile (10  $\mu\text{M}$ ) were coated on a Whatman filter paper strip ( $2 \times 1 \text{ cm}^2$ ) and dried in air. As shown in Fig. 10, when the probe-based test strips were immersed in solutions of different pH values, an instantaneous color change was observed under ultraviolet light. Therefore, probes **1a-b** have good fluorescence sensing performance in solid state, and the alkaline pH value can be easily detected by probe test paper without additional equipment.

### 3.7. Detection of pH in concrete

We used probes **1a-b** to detect the pH in concrete. For the determination, we soaked concrete in 30 ml water with different pH values (pH 8, 9, 10, 11, 12 for **1a** and pH 7, 8, 9, 10, 11 for **1b**) for 7 days, and then dried them in air. As shown in Fig. 11, when the concretes with different pH values were dipped in the solutions of probe **1a** or **1b**, an instantaneous color change can be observed under ultraviolet light. There-

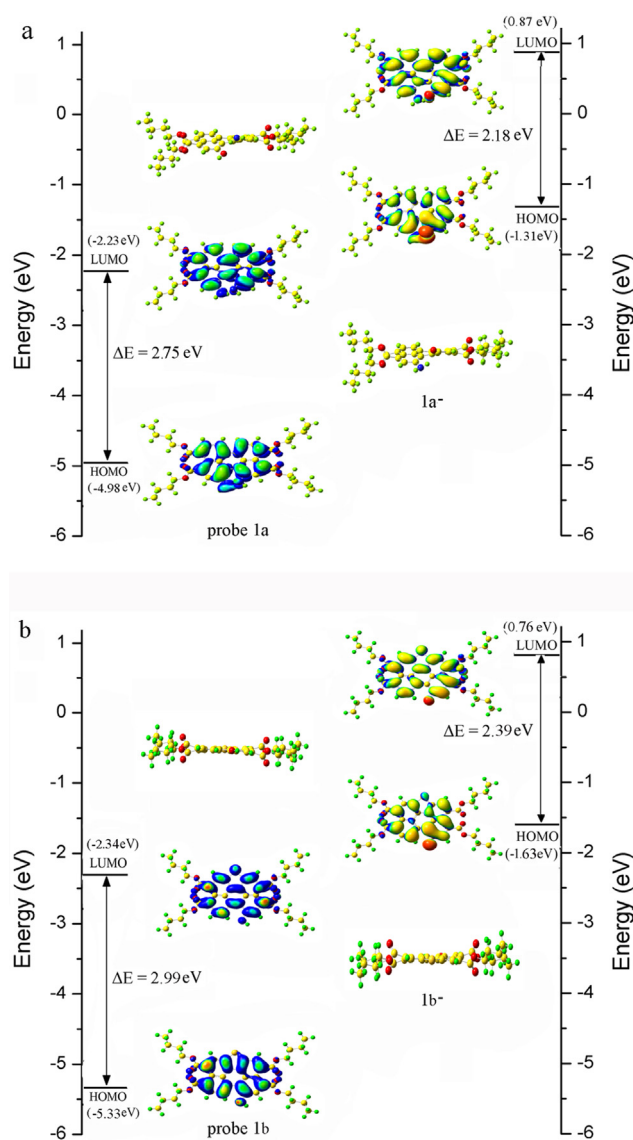


**Fig. 9** Energy diagram of HOMO and LUMO orbital of (a) probe **1a** and (b) probe **1b** and their corresponding negatively charged forms calculated at the DFT level using a B3LYP/6-31G\* basis set.

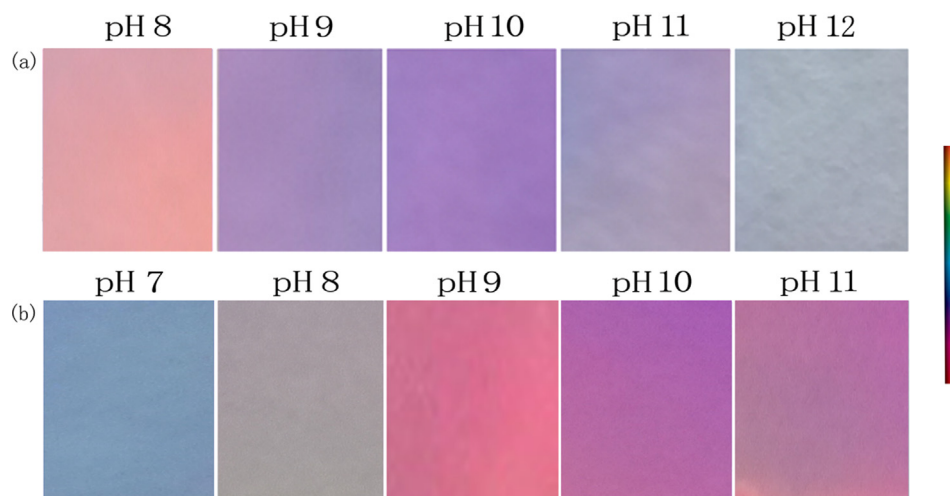
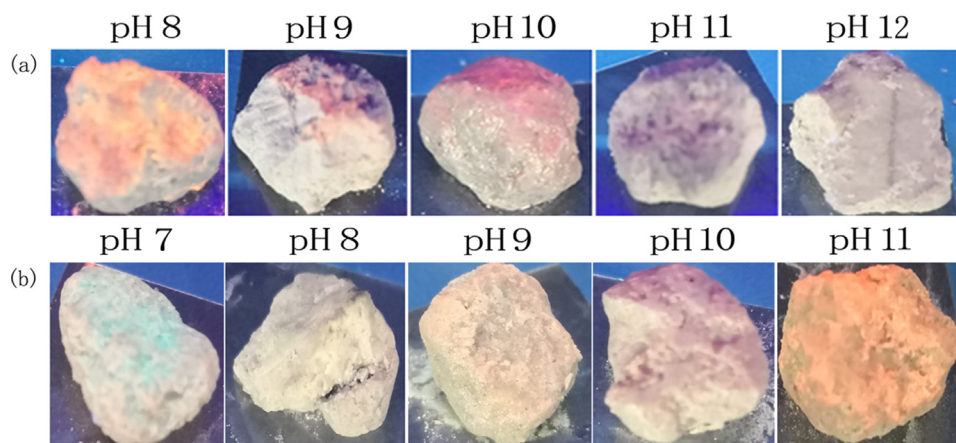
fore, probes **1a-b** could be particularly useful for the quantitative determination of pH value of concrete.

## 4. Conclusions

In this study, two fluorescent pH probes **1a-b** for alkaline pH range based on PTACs has been modified, which had different substitution patterns and induced pH responses in long wavelength and short wavelength region. Due to the protonating and deprotonating processes, probes **1a-b** had colorimetric response at 507/563 nm and 450/520 nm, respectively. The maximum peak of their emission spectra was at 582 nm and 481 nm with different Stokes shifts 75 and 31 nm. The probes had very high pKa values because of the decoupling from the electron withdrawing core of perylene. Compared with probe **1a**, probe **1b** had a lower pKa value. This suggested that

**Table 2** Calculated and experimental parameters for compounds **1a-b**, **1a<sup>-</sup>-b<sup>-</sup>**.

Compound	HOMO <sup>a</sup> (eV)	LUMO <sup>a</sup> (eV)	E <sub>g</sub> <sup>a</sup> (eV)	λ <sub>max</sub> (nm)	E <sub>g</sub> <sup>b</sup> (eV)
1a	-4.98	-2.23	2.75	503	2.47
1a <sup>-</sup>	-1.31	0.87	2.18	563	2.20
1b	-5.31	-2.35	2.96	448	2.76
1b <sup>-</sup>	-1.63	0.76	2.39	520	2.38

<sup>a</sup> Calculated by DFT/B3LYP (in eV).<sup>b</sup> At absorption maxima in aqueous solution (E<sub>g</sub> = 1240/λ<sub>max</sub>).**Fig. 10** Photographs of test strips of **1a** (a) and **1b** (b) at various pH irradiated at 365 nm with a hand-held lamp.**Fig. 11** Photographs of concretes with different pH values after been dipped in probes **1a** (a) and **1b** (b) solutions irradiated at 365 nm with a hand-held lamp.

adjustable pK<sub>a</sub> could be achieved by the modification of electron withdrawing groups. Both the two probes showed excellent solubility in organic solvents and exhibited highly reversible responses to pH. It was insensitivity for probes **1a-b** to ions such as Na<sup>+</sup>, K<sup>+</sup>, Mg<sup>2+</sup>, Ca<sup>2+</sup>, Ag<sup>+</sup>, Al<sup>3+</sup>, Ba<sup>2+</sup>, Cd<sup>2+</sup>, Co<sup>2+</sup>, Fe<sup>2+</sup>, Hg<sup>2+</sup>, Mn<sup>2+</sup>, Ni<sup>2+</sup>, Pb<sup>2+</sup>, Zn<sup>2+</sup>, Cl<sup>-</sup>, Br<sup>-</sup>, I<sup>-</sup>, NO<sub>3</sub><sup>-</sup>, H<sub>2</sub>PO<sub>4</sub><sup>-</sup>, BF<sub>4</sub><sup>-</sup>, and ClO<sub>4</sub><sup>-</sup>. They had good fluo-

rescence sensing performance in solid state, and the alkaline pH value can be easily detected by probe test paper without additional equipment. Also, the dynamic ranges of the probes could cover the typical pH changes that happening along with the corrosion and deterioration of concrete structures. It was hoped that this study would be helpful for designing and synthesizing novel fluorescent perylene probes for alkaline pH.

## Declaration of Competing Interest

There are no conflicts to declare.

## Acknowledgements

This work was supported by the Doctoral Foundation of Shandong Jianzhu University (XNBS1938, XNBS1712, XNBS1824), Science and Technology Plan Project of Housing and Urban-Rural Construction Department in Shandong Province (2018-K11-01, 2018-K7-01), Youth Innovation Technology Project of Higher School in Shandong Province (2019KJD003), Shandong Key Research and Development Program (2019GSF109064, 2019GSF109088) and National Natural Science Foundation of China (41907204).

## Appendix A. Supplementary material

Supplementary data to this article can be found online at <https://doi.org/10.1016/j.arabjc.2020.04.033>.

## References

- Aigner, D., Borisov, S.M., Petritsch, P., Klimant, I., 2013. Novel near infra-red fluorescent pH sensors based on 1-aminoperylene bisimides covalently grafted onto poly(acryloylmorpholine). *Chem. Commun.* 49, 2139–2141.
- Aulin, Y.V., Felter, K.M., Gunbas, D.D., Dubey, R.K., Jager, W.F., Grozema, F.C., 2018. Morphology-independent efficient singlet exciton fission in perylene diimide thin films. *ChemPlusChem* 83, 230–238.
- Chai, X., Cui, X., Wang, B., Yang, F., Cai, Y., Wu, Q., Wang, T., 2015. Near-infrared phosphorus-substituted rhodamine with emission wavelength above 700 nm for bioimaging. *Chem.–Eur. J.* 21, 16754–16758.
- Chao, C.C., Leung, M.K., Su, Y.O., Chiu, K.Y., Lin, T.H., Shieh, S.J., Lin, S.C., 2005. Photophysical and electrochemical properties of 1,7-diaryl-substituted perylene diimides. *J. Org. Chem.* 70, 4323–4331.
- Dubey, R.K., Inan, D., Sengupta, S., Sudholter, E.J.R., Grozema, F.C., Jager, W.F., 2016. Tunable and highly efficient lightharvesting antenna systems based on 1,7-perylene-3,4,9,10-tetracarboxylic acid derivatives. *Chem. Sci.* 7, 3517–3532.
- Georgiev, N.I., Krasteva, P.V., Bojinov, V.B., 2019. A ratiometric 4-amido-1,8-naphthalimide fluorescent probe based on excimer-monomer emission for determination of pH and water content in organic solvents. *J. Lumin.* 212, 271–278.
- Gotor, R., Ashokkumar, P., Hecht, M., Keil, K., Rurack, K., 2017. Optical pH sensor covering the range from pH 0–14 compatible with mobile-device readout and based on a set of rationally designed indicator dyes. *Anal. Chem.* 89, 8437–8444.
- Gupta, R.K., Pradhan, B., Pathak, S.K., Gupta, M., Pal, S.K., Sudhakar, A.A., 2015. Perylo[1,12-b, c, d] thiophene tetraesters: a new class of luminescent columnar liquid crystals. *Langmuir* 31, 8092–8100.
- Han, J., Burgess, K., 2010. Fluorescent indicators for intracellular pH. *Chem. Rev.* 110, 2709–2728.
- Hecht, M., Kraus, W., Rurack, K., 2013. A highly fluorescent pH sensing membrane for the alkaline pH range incorporating a BODIPY dye. *Analyst* (138), 325–332.
- Horváth, P., Šebej, P., Kovář, D., Damborský, J., Prokop, Z., Klán, P., 2019. Fluorescent pH indicators for neutral to near-alkaline conditions based on 9-iminopyronin derivatives. *ACS Omega* 4, 5479–5485.
- Inan, D., Dubey, R.K., Westerveld, N., Bleeker, J., Jager, W.F., Grozema, F.C., 2017. Substitution effects on the photoinduced charge-transfer properties of novel perylene-3,4,9,10-tetracarboxylic acid derivatives. *J. Phys. Chem. A* 121, 4633–4644.
- Li, K., Wang, J.M., Li, Y.Y., Si, Y., He, J., Meng, X.R., Hou, H.W., Tang, B.Z., 2018. Combining two different strategies to overcome the aggregation caused quenching effect in the design of ratiometric fluorescence chemodosimeters for pH sensing. *Sens. Actuators B* 274, 654–661.
- Li, C., Wonneberger, H., 2012. Perylene imides for organic photovoltaics: yesterday, today, and tomorrow. *Adv. Mater.* 24, 613–636.
- Lukinavicius, G., Reymond, L., Umezawa, K., Sallin, O., D'Este, E., Göttfert, F., Ta, H., Hell, S.W., Urano, Y., Johnsson, K., 2016. Fluorogenic probes for multicolor imaging in living cells. *J. Am. Chem. Soc.* 138, 9365–9368.
- Ma, Y.S., Shi, Z.Q., Zhang, A.D., Li, J.F., Wei, X.F., Jiang, T.Y., Li, Y.A., Wang, X.L., 2016. Self-assembly, optical and electrical properties of five membered O- or S-heterocyclic annulated perylene diimides. *Dyes Pigments* 135, 41–48.
- Ma, Y.S., Zhao, Y.L., Zhang, F.X., Jiang, T.Y., Wei, X.F., Shen, H., Wang, R., Shi, Z.Q., 2017. Two new chemosensors for fluoride ion based on perylene tetra-(alkoxycarbonyl) derivatives. *Sens. Actuators B* 241, 735–743.
- Marciniak, H., Li, X.Q., Würthner, F., Lochbrunner, S., 2011. One-dimensional exciton diffusion in perylene bisimide aggregates. *J. Phys. Chem. A* 115, 648–654.
- Myochin, T., Kiyose, K., Hanaoka, K., Kojima, H., Terai, T., Nagano, T., 2011. Rational design of ratiometric near-infrared fluorescent pH probes with various pKa values, based on aminocyanine. *J. Am. Chem. Soc.* 133, 3401–3409.
- Nguyen, T.H., Venugopala, T., Chen, S., Sun, T., Grattan, K.T.V., Taylor, S.E., Basheer, P.A.M., Long, A.E., 2014. *Sens. Actuators B* 191, 498–507.
- Rao, K.V., Haldar, R., Kulkarni, C., Maji, T.K., George, S.J., 2012. Perylene based porous polyimides: tunable, high surface area with tetrahedral and pyramidal monomers. *Chem. Mater.* 24, 969–971.
- Shoer, L.E., Eaton, S.W., Margulies, E.A., Wasielewski, M.R., 2015. Photoinduced electron transfer in 2,5,8,11-tetrakis-donor-substituted perylene-3,4,9,10-bis(dicarboximides). *J. Phys. Chem. B* 119, 7635–7643.
- Sondergaard, R.V., Christensen, N.M., Henriksen, J.R., Kumar, E.K. P., Almdal, K., Andresen, T.L., 2015. Facing the design challenges of particle-based nanosensors for metabolite quantification in living cells. *Chem. Rev.* 115, 8344–8378.
- Staudinger, C., Breininger, J., Klimant, I., Borisov, S.M., 2019. Near-infrared fluorescent aza-BODIPY dyes for sensing and imaging of pH from the neutral to highly alkaline range. *Analyst* 144, 2393–2402.
- Sukul, P.K., Datta, A., Malik, S., 2014. Light harvesting and amplification of emission of donor perylene-acceptor perylene aggregates in aqueous medium. *Chem. - Eur. J.* 20, 3019–3022.
- Vanacek, P., Sebestova, E., Babkova, P., Bidmanova, S., Daniel, L., Dvorak, P., Stepankova, V., Chaloupkova, R., Brezovsky, J., Prokop, Z., Damborsky, J., 2018. Exploration of enzyme diversity by integrating bioinformatics with expression analysis and biochemical characterization. *ACS Catal.* 8, 2402–2412.
- Wang, J., Zhong, S.L., Duan, W.F., Gao, B.X., 2015. Fluorinated perylene diimides: synthesis, electrochemical-photophysical properties, and cellular imaging. *Tetrahedron Lett.* 56, 824–827.
- Weitz, R.T., Amsharov, K., Zschieschang, U., Villas, E.B., Goswami, D.K., Burghard, M., Dosch, H., Jansen, M., Kern, K., Klauk, H., 2008. Organic n-channel transistors based on core-cyanated perylene carboxylic diimide derivatives. *J. Am. Chem. Soc.* 130, 4637–4645.
- Wenger, O.S., 2011. How donor–bridge–acceptor energetic influence electron tunneling dynamics and their distance dependences. *Acc. Chem. Res.* 44, 25–35.

- Yang, X.F., Qin, X.J., Zhu, F.Q., Shi, W.D., 2019. A through-bond energy transfer-based ratiometric fluorescent pH probe: For extreme acidity and extreme alkaline detection with large emission shifts. *Talanta* 200, 350–356.
- Yin, J., Hu, Y., Yoon, J., 2015. Fluorescent probes and bioimaging: alkali metals, alkaline earth metals and pH. *Chem. Soc. Rev.* 44, 4619–4644.
- Yuan, C.X., Li, J.Y., Xi, H., Li, Y.X., 2019. A sensitive pyridine-containing turn-off fluorescent probe for pH detection. *Mater. Lett.* 236, 9–12.
- Zhang, F.X., Ma, Y.S., Chi, Y.H., Yu, H.H., Li, Y.A., Jiang, T.Y., Wei, X.F., Shi, J.M., 2018. properties of perylene diimide dyes bearing unsymmetrical substituents at bay position. *Sci. Rep* 8, 8208–8219.
- Zhao, G.J., Han, K.L., 2009. Excited state electronic structures and photochemistry of heterocyclic annulated perylene (HAP) materials tuned by heteroatoms: S, Se, N, O, C, Si, and B. *J. Phys. Chem. A* 113, 4788–4794.